J. Indian Inst Sci., July–Aug 1989, **69**, 295–320.

IISc THESES ABSTRACTS

Thesis Abstract (Ph.D.)

Studies on B-DNA: Fibre diffraction and ligand binding by Pradipkumar Parrack.
Research supervisor: V. Sasisekharan.
Department: Molecular Biophysics Unit.

1. Introduction

This thesis consists of two parts. Part I contains X-ray fibre diffraction studies on B-DNA. Part II is concerned with the design, synthesis, and physicochemical studies of structural analogues of the oligopeptide antibiotic distamycin, a B-DNA-specific ligand.

2. Fibre diffraction of DNA

A thorough and systematic conformational analysis examining all possible helical structures for B-DNA, using the flexible mononucleotide as the building block, was first started in our laboratory[1]. As a result of such studies, several right- and left-handed models were generated, which were consistent with the then available X-ray fibre as well as IR dichroism data[2]. The author started X-ray fibre diffraction of DNA with special emphasis on the B-form. The objective was to supplement the earlier model building work with first-hand fibre data with which different possible models may be compared.

It was observed[3] that for the lithium salt of calf-thymus DNA, the diffraction pattern corresponding to the best 'crystalline B-form' cannot be explained in terms of regular helical structures. Additionally, structural transitions in the solid state, as a function of environmental conditions, were also detected highlighting the flexibility inherent in the structure, earlier indicated by conformational calculations from our laboratory.

After an examination of the existing methods for fibre preparation, a method for accurately controlling the salt content in DNA fibres (a necessary factor in determining crystallinity and nature of the X-ray pattern) was developed for the first time ever in our laboratory[3]. The procedures standardised enabled obtaining crystalline B-DNA patterns with a very high degree of reproducibility. Appearance and disappearance of meridional reflections on the fourth, sixth, and tenth layer lines indicated nonuniformity and variability in the structure[3]. This was confirmed by sensitive and quantitative measurements of helical parameters from layer-line spacings, using the precision method of X-ray diffraction, for the first time for DNA fibres[4]. Such variations being present in the best B-patterns, along with the indication of nonhelical nature of the structure, model building studies to explain all the observed data are rendered extremely difficult. It was realised that the X-ray data did not warrant such an accurate solution of the fine structure of B-DNA.

3. Ligand-binding studies

In order to study some gross features of the structure (such as handedness) and also to try to 'fix' the structure in one of its microheterogenous states, nonintercalative DNA-binding ligands, netrospin (Nt) and distamycin (Dst), were chosen as model systems. These compounds, which are naturally occurring oligopeptide antibiotics (pyrrolamides), bind to B-DNA with a high specificity toward the DNA secondary structure, AT base pairs, and the minor groove[5]. Because of their inherent structural complementarity to the B-DNA minor groove, they serve as suitable models based on which specific structural probes might be designed.

The author was involved in the initiation of such an approach to DNA structure, and the work presented in part II of the thesis comprises efforts to build up the necessary base for the same. To design structural probes, details of the specific interactions must be known. The program undertaken in our laboratory to this end is aimed at understanding the conformational and chemical basis for the specific interactions of Nt/Dst type of ligands with DNA.

An isohelical analysis on pyrrolamides was carried out with the specific objective of examining their compatibility with the B-DNA structure, and the viability of a pyrrole-β-alanine repeat unit in this regard was recognised. Two such pyrrole-β-ala-containing analogues of distamycin, PPA and PAP, were synthesised. Introduction of the saturated β-ala moiety results in a decrease in the extended conjugation (which is present *via* contiguous pyrrolamides, as in Dst). Detailed spectroscopic studies on the DNA-binding characteristics of PPA and PAP were undertaken to examine the important and hitherto unnoticed role of this extended conjugation in Dst-DNA interactions. It is shown that the loss of extended conjugation in the ligands does not influence the specificities of binding[6]. More detailed investigations reveal that such conjugation contributes to the stability of the ligand-DNA complex[7].

References

1. SASISEKHARAN, V. AND PATTABIRAMAN, N. — *Nature*, 1978, **275**, 159–162.
2. SASISEKHARAN, V., BANSAL, M. AND GUPTA, G. — In *Nucleic acids: The vectors of life* (eds B. Pullman and J. Jortner), 1983, pp. 101–111, D. Reidel.
3. PARRACK, P., DATTA, S. AND SASISEKHARAN, V. — *J. Biomol. Struct. Dynam.*, 1984, **2**, 149–157.
4. SUNDARAMOORTHY, M., PARRACK, P. AND SASISEKHARAN, V. — In *Biomolecular stereodynamics*, Vol. IV (eds R. H. Sarma and M. H. Sarma), 1986, pp. 217–225, Adenine Press, Guilderland, NY.
5. ZIMMER, C. AND WAHNERT, U. — *Prog. Biophys. Mol. Biol.*, 1986, **47**, 31–112.
6. PARRACK, P., DASGUPTA., D., AYYER, J. AND SASISEKHARAN, V. — *FEBS Lett.*, 1987, **212**, 297–301.
7. DASGUPTA., D., PARRACK, P. AND SASISEKHARAN, V. — *Biochemistry*, 1987, **26**, 6381–6386.

Thesis Abstract (Ph.D.)

Spectroscopic investigations of an antifertility agent, gossypol, and an ionophore antibiotic lasalocid A by D. S. Sampath.
Research supervisor: P. Balaram.
Department: Molecular Biophysics Unit.

1. Introduction

Low molecular weight polyfunctional organic natural products constitute a structurally diverse class of molecules which display a remarkable spectrum of biological activities. Such molecules invariably arise as secondary by-products of cellular metabolism and their precise role in the parent system remains obscure. In this study, gossypol and lasalocid A, two polyoxygenated members of this class have been subjects of detailed biophysical investigations.

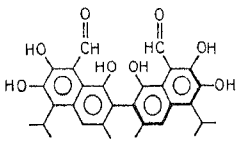

Gossypol

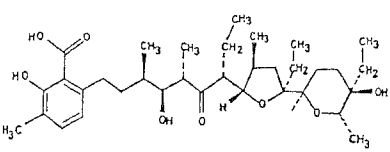

Lasalocid A

2. Experimental procedures

CD spectra were recorded on a JASCO J-20A spectropolarimeter. Fluorescence studies were performed either on a Perkin-Elmer MPF-44A spectrofluorimeter or a Hitachi 650-60 spectrofluorimeter. HPLC studies were carried out using an LKB two-pump system with a controller unit. Analyses were carried out on a Lichrosorb reverse-phase C_{18}(RP-18) column of dimension 4 × 250 mm (particle size, 10 μm) using methanol-water as the eluant. 270 MHz ^{1}H and 67.89 MHz ^{13}C NMR spectra were recorded on the Bruker WH-270 FT NMR spectrometer equipped with an Aspect-2000 computer, at the Sophisticated Instruments Facility, Indian Institute of Science, Bangalore.

(+)-Gossypol was extracted from the bark of *Thespesia populnea* by a modified procedure as described in the literature[1,2]. Amino-acid derivatives employed in the study were prepared by standard procedures and characterised. Racemic (±)-gossypol acetic acid was obtained as a gift from the National Institute of Child Health (WHO Special Program). Other chemicals were purchased from Sigma Chemical Company, USA.

3. Main results and conclusions

The CD spectral investigations of (+)-gossypol reveal a rich spectrum spanning the range 200–450 nm (fig. 1). There are five principal CD bands situated at ~ 370 nm (positive; band I), ~ 340 nm (negative; band II), ~ 300 nm (negative; band III), ~ 270 nm (positive; band IV) and ~ 230 nm (negative; band V). Bands I, IV and V are characterised by high ellipticities whereas bands II and III exhibit low ellipticities. Band assignments have been made based on the known electronic transitions

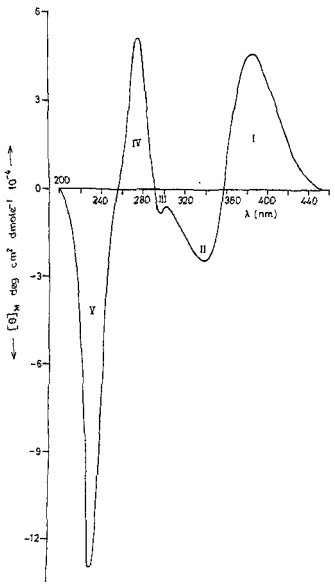

FIG. 1. CD spectrum of (+)-gossypol (50 μM) in ethanol. Path length, 0.5 cm.

of 2,2'-binaphthyl[3], the principal chromophore in gossypol. Band I has been assigned to the $^1L_b \leftarrow {}^1A$ transition, band III to the $^1L_a \leftarrow {}^1A$ transition, band IV to the $^1B_b \leftarrow {}^1A$ transition and band V to the $^1C_b \leftarrow {}^1A$ transition. Band II for which there is no clearly distinguishable UV absorption maximum has been assigned to the $n \rightarrow \pi^*$ carbonyl transition. These results have been extended to use gossypol as a CD probe of protein-binding sites.

Optical resolution of racemic (±)-gossypol has been accomplished using a variety of chiral amino compounds. These include L-phenylalaninol, (−)-norepinephrine, (−)-epinephrine, D-glucosamine, D-galactosamine, D-mannosamine and a dilysine tetrapeptide Boc-Lys-Pro-Aib-Lys-NHMe. Separation of the diastereomeric complexes of (±)-gossypol with the chiral amines is achieved by HPLC on an *achiral phase* column with methanol-water mixtures of varying composition as the eluant. (−)- or (+)-gossypol can be easily prepared by acid hydrolysis of the respective resolved gossypol adducts. The present procedures differ from the two other procedures published recently[4,5] in the following respects: (i) Both the component enantiomers, (+)- and (−)- of gossypol, could be obtained in good yields from an individual run. (ii) An *achiral column* suffices to yield a good resolution.

Representative examples depicting the good resolutions obtained are presented in fig. 2.

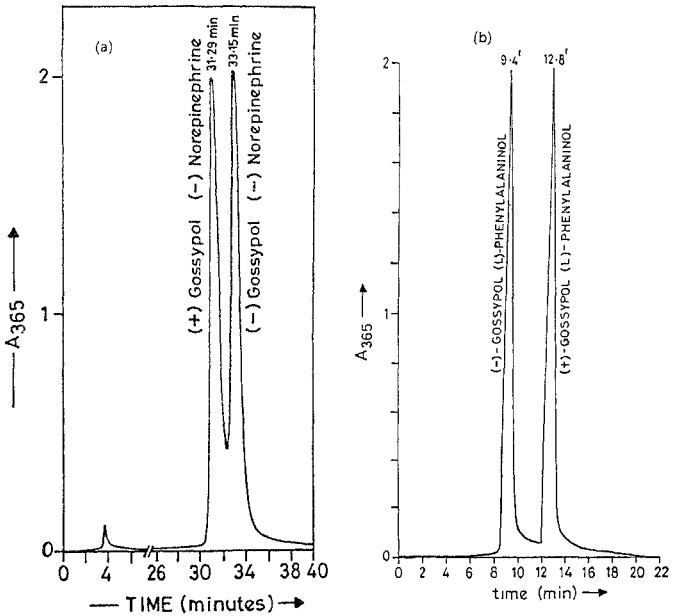

FIG. 2. HPLC trace of (a) (±)-gossypol—(−)-norepinephrine adduct and (b) (±)-gossypol—L-phenylalaninol adduct. Column: Lichrosorb RP-18 (4 × 250 mm, 10 μm particle size). Retention time is indicated against the peaks. Detection by UV absorption at 365 nm. Elution: (a) Gradient elution with 67–83% MeOH-H_2O in 35' followed by 83–95% MeOH-H_2O in 3'; (b) Gradient elution with 90–95% MeOH-H_2O in 15'.

In low concentration regimes (gossypol, $\leqslant 50\,\mu$M; protein, $\leqslant 50\,\mu$M) there are no large changes in the CD spectrum of (+)-gossypol on binding to serum albumins. But under high concentration conditions (gossypol, $\geqslant 100\,\mu$M; protein, $\geqslant 100\,\mu$M) large changes are observed. Under these conditions 'induced CD' spectra have been observed for racemic (±)-gossypol in the case of HSA and BSA (fig. 3). The spectral characteristics are different for the two proteins. Differential perturbation of the bound-gossypol enantiomers is thought to be responsible for such 'induced CD' spectra.

All the three gossypol forms (+)-, (−)- and (±) interact with artificial lipid membranes and affect lipid-phase fluidity. At low concentrations (mole ratios < 0.05 with respect to lipid) gossypol has an ordering effect on the membrane lipids, whereas at high concentrations (mole ratios 0.05–0.25, examined in this study) it has a disordering effect. A significant feature of the studies under high concentration conditions is the enantiomeric difference for the gossypol-induced fluidity changes.

The aqueous-phase CD studies of lasalocid A suggest it exists in an open, extended quasilinear

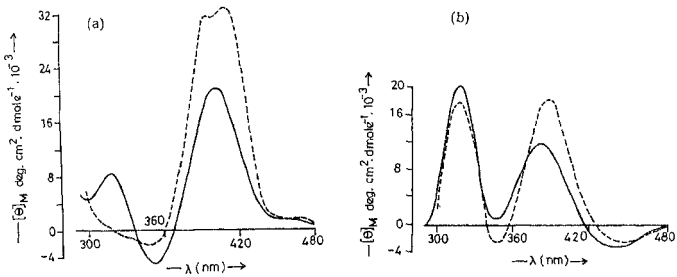

FIG. 3. Induced CD spectra of (±)-gossypol (335 μM) in the presence of (a) HSA (289 μM) in phosphate buffer (1 mM, pH 7.0) and, (b) BSA (289 μM) in phosphate buffer (1 mM, pH 7.4).—Spectra recorded immediately after mixing; ---spectra recorded after 72 h of incubation.

conformation under such conditions. The resultant exposure of apolar side chains and hence unfavourable interactions are suggested to be offset by aggregation of the ionophore into small micellar structures. In micelles and phospholipid dispersions the ionophore appears to largely favour an extended quasilinear conformer. Fluorescene polarisation studies of lasalocid A in water indeed suggest aggregate structures with the aggregation number being ~ 30. This observation finds further support from gel filtration studies which yield an $M_r \simeq 18{,}000$ for the molecular species of the ionophore prevalent in water. Based on fluorescence studies an estimate of 0.04 μM has been arrived at for the critical micellar concentration.

References

1. KING, T. J. AND DE SILVA, L. B. — *Tetrahedron Lett.*, 1968, 261–263.
2. DATTA, S. C., MURTI, V. V. S. AND SESHADRI, T. R. — *Curr. Sci.*, 1968, **37**, 135.
3. JAFFE, H. H. AND ORCHIN, M. — *Theory and applications of ultraviolet spectroscopy*, 1962, Wiley.
4. ZHENG, D. K., SI, Y. K., MENG, J. K., ZHOU, J. AND HUANG, L. — *J. Chem. Soc., Chem. Commun.*, 1985, 168–169.
5. MATLIN, S. A., ZHOU, R., BIALY, G., BLYE, R. P., NAQVI, R. H. AND LINDEBERG, M. C. — *Contraception*, 1985, **31**, 141–149.

Thesis Abstract (Ph.D.)

Altered conformations in natural DNA: Studies on supercoiled form V DNA by Yogesh S. Shouche.
Research supervisor: S. K. Brahmachari.
Department: Molecular Biophysics Unit.

1. Introduction

The demonstration of sequence-dependent conformational flexibility of DNA[1] and the discovery of left-handed Z-DNA[2] paved the way for a detailed study on the possible role for such structures of DNA. So far the studies were restricted to synthetic oligo and polynucleotides with very little focus on naturally occurring sequences. In the present work, attempt has been made to identify the sequences that have a potential to adopt unusual structures under the topological stress, which is known to play an important role in gene regulation *in vivo*. Supercoiling is also known to be an important factor in inducing structural alteration in alternating purine-pyrimidine sequences cloned in circular plasmids.

Form V DNA, prepared by reannealing of two single-stranded complementary circles[3,4], was used as a model system. In this molecule, due to topological constraint, every right-handed turn is compensated by a left-handed turn or negative supercoiling; as a result up to 40% of the molecule adopts unusual (non-B) conformation[5,6]. In this work, such unusual structures were characterised, their interaction with structure-specific antibodies and transacting factors like Z-DNA binding protein was also investigated. In addition, sequences that adopt unusual structure were mapped using sequence-specific enzymes like restriction endonucleases and modification methylases. This provided detailed information as to the role of neighbouring sequences on supercoil-induced structural transition in DNA.

2. Materials and methods

All the reagents were of Analar grade. Restriction endonucleases and methylases were from New England Biolabs. UV, CD and sedimentation analyses were performed on Beckman DU-8B spectrophotometer, JASCO-J500 spectropolarimeter and Beckman analytical ultracentrifuge, respectively.

Plasmids were purified by CsCl-Etbr density-gradient centrifugation and by the method developed in our laboratory. Z-DNA antibody raised against Z form of poly (dG-dC) was a gift from Prof. B. D. Stollar. Preparation and purification of pBR322 form V DNA, antibody-binding, 2-D gel electrophoresis restriction endonuclease digestion and methylation experiments were carried out as described earlier[4,7].

3. Results and discussion

3.1. *Preparation and purification of form V DNA*

Form V DNA was prepared following the method of Stettler *et al*[3]. They used DNase I digestion of plasmid in the presence of ethidium bromide (300 μg/ml) to get form II DNA having single nick per molecule. Since DNase I cleavage is difficult to control, a new method involving EcoRI digestion in the presence of ethidium bromide (400 μg/ml) was developed taking advantage of the fact that EcoRI has a single cleavage site in pBR322. Form V DNA prepared from pBR322 and pBG plasmids gave a

sharp band on electrophoresis indicating the homogeneous nature of the folded molecule during reannealing It showed a faster electrophoretic mobility than form I DNA indicative of higher supercoiling. The yield of form V DNA was found to be 10% of the starting plasmid.

3.2. *Characterisation of form V DNA*

A detailed characterisation of form V DNA prepared from plasmids pBR322 and pBG was carried out. Two-dimensional gel electrophoresis and sedimentation analyses showed that form V DNA is a highly compact supercoiled molecule. Thermal denaturation and circular dichroism studies suggest that up to 35–40% of the sequences are present in the left-handed helical conformation. Studies using Z-DNA-specific protein and antibody indicate that a major portion of the altered structures in form V DNA probably have a left-handed Z conformation. These structures were found to be stabilised by multivalent cations like hexamine cobalt chloride and destabilised by DNA unwinding agents like ethidium bromide.

A search of the complete sequence of pBR322 shows that there are very few alternating purine-pyrimidine sequences, which implies that in form V DNA due to zero link, sequences other than these must be adopting Z-like left-handed helical conformations. Probing the structure adopted by different sequences in form V DNA may reveal the possible conformation that various sequences are capable of adopting under the topological stress.

3.3. *Probing of altered structures using single-cut restriction endonucleases*

Sequences that adopt unusual structures in form V DNA were mapped using restriction endonucleases, that have single cleavage site in pBR322, as probes. ClaI, EcoRV, EcoRI, SalI, SphI and PvuII sites were completely cleaved, whereas BamHI, AvaI, PstI, HindIII sites showed resistance to cleavage. These resistant sites became amenable to cleavage after removal of topological strain either by cleavage with other restriction endonucleases or topoisomerase I.

Analysis of flanking sequences at these resistant sites revealed the presence of poly pyrimidine-poly purine stretches or short stretches of alternating purine-pyrimidine sequences (a few bases out of alternation in some cases) at these locations. These sequences are known to adopt altered conformation under the force of supercoiling[8,9]. Such sequences may be influencing the structure adopted by restriction endonuclease recognition sequence. Using this approach the enzyme recognition sites were divided into two groups: (i) sequences that are cleavable in form V DNA, including those that adopt B or B-DNA-like conformation, and (ii) sequences that are uncleavable by restriction endonucleases. The latter includes Z-DNA, single-stranded DNA and other non-B structures.

3 4. *Probing of altered structures using multiple-cut restriction endonucleases*

Since the single-site enzymes give information about a very small portion of the molecule, the studies were extended to the enzymes with multiple sites in pBR322. A single hit approach was used to retain the topological strain at the time of cleavage so that the topological strain would be retained while the enzymes cleave at each of the sites.

All the four sites of enzyme NarI (GGCGCC) and FspI(TGCGCA) showed reduced rate of cleavage in form V DNA as compared to form I DNA. NarI recognition sites 434 and 548 showed significant resistance to cleavage. These contain an 8-bp alternating purine-pyrimidine sequence and a

poly purine-poly pyrimidine stretch, respectively, in the flanking region.

Similarly FspI site 1454 that showed resistance to cleavage in form V DNA contained a large stretch of alternating purine-pyrimidine sequence. Thus, similar hexanucleotide sequences could adopt different conformations depending on the flanking sequence under identical topological strain.

3.5. *Probing of altered structures using sequence-specific methylases*

Geometry of the Z-DNA makes 5′ position of the cytosine unavailable for methylation by methylases[10]. This fact was used to map Z-DNA and other unusual structures present in form V DNA. This technique has an advantage over those described earlier because the sequence is modified rather than cleaved. Hence, the history of the structure of methylatable sites is preserved as a methylation level even when the superhelical strain in form V is removed by subsequent restriction endonuclease cleavage. Extent of methylation of various sites was quantitated by incorporation of ^{3}H methyl groups using ^{3}H SAM as substrate for methylases followed by fluorography. After complete or near-complete methylation, all the five methylases tested were found to methylate form V DNA to a significantly lower level compared to form I DNA. One methylase (M. HhaI) recognising alternating purine-pyrimidine sequence (GCGC) and another (M. AluI) recognising non-alternating sequence (AGCT) were used to rank their cognate methylation sites based on the extent to which they are methylatable.

Some sequences in form V were shown to be completely in B form while others exist partly in altered conformation. Modulation effect of neighbouring sequences was seen as not all the potential Z-forming sequence (alternating purine pyrimidine) of less than 7 bp adopt Z conformation in form V DNA. Regions of imperfect alternating purine-pyrimidine structure were sometimes capable of adopting altered conformation; and poly purine-poly pyrimidine stretches were found to be the second best candidates to adopt unusual structure. In addition, some regions of altered structure had no apparent Z-forming sequence, nor were they in polypurine stretches. These might represent novel left-handed helical structures. Large regions of either B or non-B conformation were not always observed. This was in contrast to the belief that B-Z junctions require a large amount of energy and hence long stretches of altered and unaltered conformations would be favoured over short stretches as they involve less number of junctions.

4. Conclusions

Using topologically constrained form V DNA as a model system, a detailed study was carried out to look at the probable structure that natural sequence could adopt under high torsional stress. It could be demonstrated that the capacity to flip over to non-B conformation was highly influenced by the nature of the flanking sequence. Sequences other than alternating purine-pyrimidine could adopt non-B conformation, presumably left-handed. Drawing the results from restriction endonuclease cleavage and methylation studies a hierarchy of altered conformations adopted by DNA sequences in form V was worked out and a map indicating the regions with structural alterations was developed. We could demonstrate that DNA topology could play a significant role in modulating sequence-dependent conformational transitions and that both right- and left-handed helical segments can coexist. Most interestingly altered and unaltered conformations appear to alternate four times in less than 40 nucleotides in the regulatory region of pBR322. Such an altered conformation in the tet^R promoter was shown to inhibit transcription initiation. The combined effect of flanking sequences and negative supercoiling has a strong effect on structure adopted by a given sequence. Thus formation of unusual structures may play an important role in the regulation of genetic processes *in vivo*.

References

1 SASISEKHARAN, V., BANSAL, M., BRAHMACHARI, S. K. AND GUPTA, G. — *Proc. Second SUNYA Conservation in the Discipline of Biomolecular Stereodynamics*, 1981, Vol. 1, p. 123, Adenine Press, New York.

2. RICH, A., NORDHEIM, A. AND WANG, A H.-J. — *Annu. Rev. Biochem.*, 1984, **53**, 791–846.

3. STETTLER, U. H., WEBER, H., KOLLER, T. H. AND WEISSMAN, CH. — *J. Mol. Biol.*, 1979, **131**, 21–40.

4. SHOUCHE, Y. S., LATHA, P. K., RAMESH, N , MAJUMDER, K., MANDYAN, V. AND BRAHMACHARI, S. K. — *J. Biosci.*, 1985, **8**, 563–578.

5. BRAHMS, S., VERGNE, J. AND BRAHMS, J. G. — *J. Mol. Biol.*, 1982, **162**, 473–493.

6. POHL, F M., THOMAE, R. AND DICAPUA, E. — *Nature*, 1982, **300**, 545–546.

7. BRAHMACHARI, S. K., SHOUCHE, Y. S., CANTOR, C. R. AND MCCLELLAND, M. — *J. Mol. Biol.*, 1987, **193**, 201–211.

8. NORDHEIM, A., LAFER, E. M., PECK, L. J., WANG, J. C., STOLLAR, B. D. AND RICH, A — *Cell*, 1982, **31**, 309–318.

9. EFSTRATIADIS, A. AND CANTOR, C. R. — *Nucleic Acids Res.*, 1984, **12**, 8059–8072.

10. VARDIMON, L. AND RICH, A. — *Proc. Natn. Acad. Sci., USA*, 1984, **81**, 3268–3272.

Thesis Abstract (Ph.D.)

Studies on riboflavin-carrier proteins: Physicochemical, biosynthetic and immunological aspects by Sandhya Visweswariah S.
Research supervisor: P. R. Adiga.
Department: Biochemistry.

1. Introduction

The mechanism of transport of water-soluble vitamins to the developing mammalian foetus has been little understood, but the discovery of certain vitamin-carrier proteins, and their obligatory requirement during pregnancy in rodents[1], suggests that a mechanism analogous to the avian system is operative in higher animals as well. Thus, a riboflavin-carrier protein (RCP) has been identified in the chicken egg and it has been shown to be involved in providing the vitamin to the developing chick embryo[2]. Antibodies to the chicken egg white RCP could detect an immunologically cross-reacting protein in pregnant rat serum, and immunoneutralisation of rat RCP was shown to lead to pregnancy

termination in the pregnant rat[1]. The studies detailed herein are concerned with the detection and subsequent characterisation of RCPs in pregnant primate sera, and a study of their biosynthetic and molecular characteristics. The fact that these primate RCPs showed immunological cross-reactivity with chicken RCP prompted the production of monoclonal antibodies (MAbs) to chicken RCP and their subsequent characterisation and study of their cross-reactivity patterns with the primate RCPs.

2. Experimental procedure

Chicken RCP was purified by the reported procedures and radioimmunoassay was performed as described earlier[3]. Primate RCPs were isolated from pregnant bonnet monkey serum and pregnant human and umbilical cord sera by high-resolution protein purification techniques such as fast-protein liquid chromatography and affinity chromatography. The isolated proteins were employed in radioimmunoassay and riboflavin-binding studies as described earlier[4].

Studies on the hormonal modulation of monkey RCP were performed on bonnet monkeys of the Institute colony. Human sera was obtained from voluntary female donors. Serum samples were assayed for RCP by a heterologous radioimmunoassay, and steroids by standardised methods[4].

Monoclonal antibodies to chicken RCP were raised by the hybridoma technique of Köhler and Milstein[5]. Characterisation of these MAbs was performed by established procedures[6], and epitope analysis performed by solid-phase binding assays[7] and a novel method developed in this thesis involving high-resolution gel filtration.

3. Main results and conclusions

Initial studies were directed towards the identification of RCPs in pregnant primate sera. Thus, by employing a heterologous radioimmunoassay utilising ^{125}I-labelled chicken RCP and its antiserum, proteins showing immunological cross-reactivity with chicken RCP were detected in pregnant bonnet monkey sera and human sera. The cross-reacting proteins were barely detected in the sera of male animals suggesting a role for them during pregnancy alone, in a manner analogous to rodent RCP.

Monkey RCP was shown to bind riboflavin with high affinity, and it was isolated by a series of gel filtration, ion-exchange, and chromatofocusing techniques. The protein was shown to have properties very similar to chicken RCP, such as molecular weight ($\sim$ 37,000) and pI ($\sim$ 4), and both primate and chicken RCPs had very similar tryptic peptide maps indicating their close sequence homology.

Human RCP was also isolated along similar lines both from human pregnancy and cord sera. These proteins had similar properties to monkey and chicken RCP, and showed a preferential affinity for riboflavin than FMN and FAD. This evolutionary conservation of RCP from birds to primates, both in terms of structure and function, suggests the vital role these proteins may have to play during gestation in higher mammals as well.

Both chicken and rat RCP have been shown to be estrogen-dependent gene products[1]. In order to study the hormonal modulation of primate RCPs, circulatory concentrations of monkey RCP were monitored during the menstrual cycle and early pregnancy of bonnet monkeys. Consequent to a mid-cycle surge of estrogen, circulatory concentrations of RCP were increased around days 16–18 of the cycle, as well as in early pregnancy. In fact, higher concentrations of RCP could be detected in circulation of immature male and female monkeys following estrogen administration to these animals, in a manner analogous to rat and chicken RCP[1]. This estrogen-dependent synthesis of monkey RCP again hints at the importance of this protein during pregnancy in monkeys.

Human RCP levels were measured in the sera of female volunteers during the menstrual cycle.

Concomitant with the two elevations of estrogen concentration during the cycle, two peaks of RCP were also observed, again suggesting the estrogen-dependent synthesis of human RCP as well.

The extensive similarities between chicken RCP and primate RCP suggested close amino-acid sequence homology amongst the proteins, and their immunological cross-reactivity was further probed by generating MAbs to chicken RCP. Optimal immunisation protocols and fusion conditions were standardised and as a result, six MAb-secreting cell lines were obtained. The MAbs were characterised with respect to sub-class, isotype and light chain type, and the affinities of the antibodies to chicken RCP estimated by a Scatchard analysis. These six MAbs were directed to three different epitopes on chicken RCP, as detected by an epitope analysis. A novel method of epitope analysis was standardised and involved high-resolution gel filtration employing Superose 12 in conjunction with fast-protein liquid chromatography. The results obtained with this method were confirmed by the routine solid-phase binding assay. By employing a radioimmunoassay utilising these MAbs and ^{125}I-chicken RCP, it was shown that the three epitopes defined by these MAbs on chicken RCP were present on both monkey and human RCP. Evidence was also obtained suggesting the identity of RCP from human pregnancy sera and umbilical cord sera. However, certain epitopes have diverged more than others during evolution as suggested by the lower affinities of primate RCPs for certain MAbs. These results thus confirm the observations made in the first chapter of the thesis as to the high degree of evolutionary conservation of RCPs, and strongly suggests that the protein-mediated vitamin delivery mechanism is operative as in lower mammals.

References

1. ADIGA, P. R. AND MURTY, C. V R. In *Molecular biology of egg maturation*, CIBA Foundation Symposium, 1983, **98**, 111–136, Pitman, London.
2. WINTER, W. P., BUSS, E G., CLAGETT, C. O. AND BOUCHER, R. V. *Comp. Biochem. Physiol.*, 1967, **22**, 897–906.
3. MURTHY, U S. *Studies on riboflavin binding protein: physicochemical and biosynthetic aspects*, Ph.D. Thesis, Indian Institute of Science, Bangalore, India, 1977.
4. MURTY, C. V. R. *Studies on vitamin carrier proteins: physicochemical, biosynthetic and functional aspects*, Ph.D. Thesis, Indian Institute of Science, Bangalore, India, 1982.
5. KOHLER, G. AND MILSTEIN, C. *Nature* (Lond.), 1975, **256**, 495.
6. GALFRÉ, G. AND MILSTEIN, C. *Methods Enzymol.*, 1981, **77**, 3–46.
7. STAHLI, C., STAEHELIN, TH. AND MIGGIANO, V. *Methods Enzymol.*, 1983, **92**, 26–36.

Thesis Abstract (Ph.D.)

Functional and structural analysis of soybean agglutinin by Musti Joginadha Swamy.
Research supervisor: A. Surolia.
Department: Molecular Biophysics Unit.

1. Introduction

Lectins are cell agglutinating and carbohydrate-binding proteins of plant and animal origin[1]. Though first discovered in the late nineteenth century, research on lectins gained momentum only in the 1940s when it was shown that certain lectins agglutinate human blood groups in a selective manner. Two observations made in the 1960s that (i) certain lectins induce mitogenicity in lymphocytes, and (ii) certain lectins preferentially agglutinate transformed cells as compared to their normal counterparts, led to the widespread use of lectins as tools in biology and medicine. In addition, the use of lectins in the purification and characterisation of glycoconjugates and carbohydrates is being widely exploited. These applications provided the impetus to the purification and characterisation of lectins from a variety of sources.

Soybean agglutinin (SBA) is an N-acetylgalactosamine-specific, homotetrameric glycoprotein isolated from the seeds of *Glycine max*[2]. This lectin attracted much attention due to its biological properties which include mitogenicity, preferential agglutination of transformed cells, a specific recognition of nodulating *Rhizobium* strains and fractionation of cells. Though a great deal of knowledge has accumulated on biological properties of SBA, which are manifested by its ability to bind to sugars, studies reporting the specificity and mechanism of its interaction with various saccharides are scarce. We have, therefore, undertaken a detailed thermodynamic and kinetic analysis of saccharide binding to this lectin.

2. Results and discussion

2.1. *Thermodynamic studies on saccharide binding to soybean agglutinin*

Thermodynamic studies on saccharide binding to SBA have been performed using fluorescence spectroscopy[3]. Binding of N-dansylgalactosamine (DnsGaln) to SBA resulted in a large increase in the fluorescence intensity of the sugar, with a concomitant blue shift of 25 nm in the emission maximum. The change in fluorescence intensity and the accompanying blue shift are due to saccharide-specific binding of the sugar to the lectin since addition of N-acetylgalactosamine reversed both the effects. By monitoring the flourescence changes observed when the sugar was titrated with the lectin, association constants for the binding of DnsGaln to SBA were determined. From the temperature dependence of the association constants (using van't Hoff plots) the thermodynamic parameters associated with the binding were calculated. Binding of non-fluorescent, inhibitory saccharides was studied by monitoring their ability to displace DnsGaln from its complex with the lectin. This study shows that in the galactose configuration, C-2 and C-6 hydroxyl groups favour the binding. A hydrophobic substituent at the anomeric position favours binding considerably. The increase in the fluorescence intensity upon binding and the blue shift in emission maximum indicate that the binding region of SBA is considerably apolar. Thermodynamic parameters obtained for the binding of DnsGaln reveal that the strong binding of this sugar ($K_a = 1.5 \times 10^6\,M^{-1}$) is due to a small entropy value ($\Delta S = -10.9\,kJ\,mol^{-1}\,K^{-1}$). Binding of simple saccharides is mainly governed by enthalpic forces.

2.2. *Kinetic studies on saccharide binding to SBA*

Stopped-flow fluorescence and temperature-jump relaxation studies have been performed to study the kinetics of saccharide binding to SBA. In the stopped-flow studies increases in the flourescence intensity of DnsGaln upon its binding to SBA was monitored as a function of time. Decrease in the fluorescence intensity of this sugar due to the dissociation of the protein-sugar complex when it was subjected to temperature perturbation was followed in the T-Jump studies. These studies show that binding of DnsGaln to SBA is a slow process ($k_{+1} = 2.4 \times 10^5\ M^{-1}\ s^{-1}$ at 20°C) which is slower than diffusion-controlled processes by 3–4 orders of magnitude. The dissociation of this complex with the rate constants of $0.2\ s^{-1}$ at 20°C is one of the slowest observed for lectin-sugar interactions[1,3].

2.3. *Chemical modification and fluorescence-quenching studies*

Chemical modification and fluorescence-quenching studies were carried out to investigate the involvement of tryptophan residues in the activity of SBA. Modification of tryptophan residues with N-bromosuccinimide (NBS) resulted in a loss of saccharide binding and hemagglutinating activities of the protein. Modification did not result in any change in the secondary structure of the protein or its state of aggregation as observed from the CD spectra and gel filtration profiles, respectively. Fluorescence quenching by iodide ion showed that some of the tryptophan residues become less accessible to the quencher in the presence of specific sugars like N-acetylgalactosamine. Kinetics of tryptophan modification by NBS, using stopped-flow spectrophotometry showed that there are two types of tryptophan residues in SBA, which are accessible to the reagents with their rate constants differing greatly from each other. In the presence of near-saturating concentrations of N-acetylgalactosamine, the kinetic data yielded three components suggesting that saccharide binding leads to an increased heterogeneity of tryptophan exposure. The kinetic data support the involvement of tryptophan residues in the activity of SBA.

2.4. *Studies on the secondary structure of SBA*

Prediction of secondary structure[4] of SBA and its comparison with that of three other legume lectins, *viz.*, Concanavalin A, *Vicia faba* lectin (Favin) and lentil lectin (LcL) show that β-pleated sheet and β-turn are the predominant secondary structural elements in these lectins. The gross secondary structural content of these lectins is very similar. They contain about 35–45% β-turn, 40–50% β-sheet and 0–10% α-helix and thereby fall into a structurally distinct class of proteins with high β-sheet and β-turn content. However, a comparison on a residue-to-residue basis showed that there is a considerably greater similarity in the secondary structure of SBA and Con A and between Favin and LcL than in other pairs suggesting a divergence in the evolution of these lectins[5].

2.5. *Chemical cross-linking studies*

Chemical cross-linking studies have been performed[6] to understand the arrangement of subunits in soybean and peanut agglutinin. Cross-linking of these homotetrameric proteins with bifunctional reagents such as dimethyl suberimidate resulted in the formation of covalently coupled oligomeric species. The products formed were analysed by polyacrylamide gel electrophoresis in the presence of sodium dodecylsulphate. The analysis of the relative content of the oligomeric species showed that in both soybean and peanut agglutinin[7] the subunits are associated in an isologous fashion (in which there is more than one type of subunit approach). The proteins have a D_2 symmetry.

References

1. SHARON, N AND LIS, H. *Annu Rev. Biochem.*, 1986, **55**, 35–67.
2. LOTAN, R., SIEGELMAN, H. W., LIS, H. AND SHARON, N. *J. Biol. Chem.*, 1974, **249**, 1219–1224.
3. SWAMY, M. J., SASTRY, M. V. K., KHAN, M I. AND SUROLIA, A. *Biochem. J.*, 1986, **234**, 515–522.
4. CHOU, P. Y. AND FASMAN, G. D. *Adv. Enzymol.*, 1978, **47**, 45–148.
5. SWAMY, M. J., SASTRY, M. V. K. AND SUROLIA, A. *J Biosci.*, 1985, **9**, 203–212.
6. HAJDU, J., BARTHA, F. AND FRIEDRICK, P. *Eur. J. Biochem.*, 1976, **68**, 373–383.
7. SALUNKE, D. M., SWAMY, M. J., KHAN, M. I., MANDE, S. C., SUROLIA, A. AND VIJAYAN, M. *J. Biol. Chem.*, 1985, **260**, 13576–13579.

Thesis Abstract (Ph.D.)

High-pressure and thermal studies on germanium and silicon telluride glasses by S. Asokan.
Research supervisor: E. S. R. Gopal.
Department: Physics.

1. Introduction

Germanium and silicon chalcogenide glasses have extensive technological applications[1]. It is highly desirable to understand the physical properties of these materials to characterise them for device applications. In the present study, response to high pressure and thermal crystallisation behaviour of germanium and silicon telluride glasses was investigated. Such studies throw light on the structure, electronic properties and their dependence on composition of chalcogenide glasses[2–4].

2. Experimental programme

Bulk Ge_xTe_{100-x} and Si_xTe_{100-x} glasses have been prepared by the melt-quenching technique. Appropriate amounts of the constituent elements (5 N purity) are sealed in fused silica ampoules (evacuated to 10^{-6} and filled with commercial argon gas). The ampoules were kept in a rotary furnace at the desired temperature and rotated continuously to homogenise the melt. After a thorough homogenisation of the alloy in the molten state for about 48 hours, the ampoules were quenched in ice water or NaOH + ice-water mixture. The glassy nature of the samples is confirmed by X-ray diffraction.

The electrical resistivity measurements at high pressures were carried out in a Bridgman anvil device up to a pressure of 8 GPa and down to liquid nitrogen temperature. The details of the experimental set-up and the calibration methods have been discussed elsewhere. Structural studies were also performed on samples recovered from the pressure cell.

The differential scanning calorimetric studies were performed on a Perkin-Elmer DSC-2 differential scanning calorimeter. These experiments are done at a constant heating rate of 20 K min^{-1}. Structural studies were carried out on a Philips X-ray diffractometer.

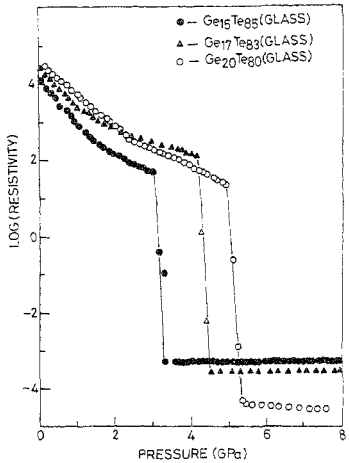

FIG. 1. The variation of electrical resistivity with pressure for $Ge_{15}Te_{85}$, $Ge_{17}Te_{83}$ and $Ge_{20}Te_{80}$ glasses.

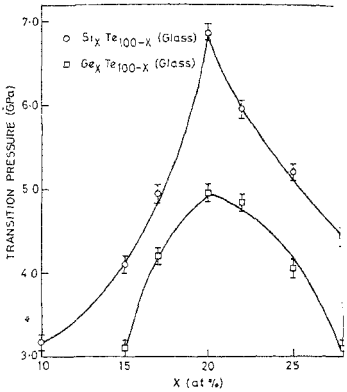

FIG. 2. The variation of transition pressure (P_T) with composition for Ge_xTe_{100-x} and Si_xTe_{100-x} glasses.

3. Main results and conclusions

The variation of electrical resistivity with pressure for Ge_xTe_{100-x} glasses with $x \leqslant 20$ is shown in fig. 1, indicating that the electrical resistivity of these glasses decreases with pressure up to a certain pressure P_T. At P_T there is a sharp, discontinuous transition from the glassy semiconductor to crystalline metal states. The behaviour is similar for all other glasses in the Ge-Te and Si-Te systems with marginal differences[5,6]. The most interesting aspect is the variation of the transition pressure P_T of Ge_xTe_{100-x} and Si_xTe_{100-x} glasses with composition x (shown in fig. 2). It is seen from fig. 2 that P_T *vs* x curve of Ge_xTe_{100-x} and Si_xTe_{100-x} glasses shows a maximum at $x \approx 20$.

The dc conductivity measurements on these glasses confirm that the material is semiconducting with a single activation energy ΔE below P_T and exhibits a metallic behaviour above P_T. The variation of ΔE as a function of x in both Ge_xTe_{100-x} and Si_xTe_{100-x} glasses shows an anomaly at the $x = 20$ composition. Figure 3 shows the variation of ΔE with x for Ge_xTe_{100-x} glasses. The E *vs* x curve of Si_xTe_{100-x} glasses is similar.

The thermal crystallisation studies on Ge_xTe_{100-x} and Si_xTe_{100-x} glasses also reveal an interesting feature at the $x = 20$ composition. Ge_xTe_{100-x} and Si_xTe_{100-x} glasses with $x \leqslant 20$ show a double-glass transition and double-stage crystallisation. On the other hand, the glasses with $x > 20$ exhibit a single-glass transition and single-stage crystallisation only[7,8].

The present high pressure and thermal crystallisation studies also reveal the existence of metastable

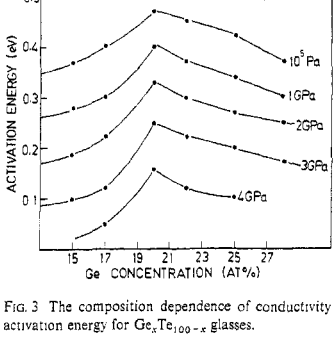

FIG. 3 The composition dependence of conductivity activation energy for Ge_xTe_{100-x} glasses.

crystalline compounds in the Ge-Te and Si-Te systems.

The important conclusions of the present studies are:

(i) Ge_xTe_{100-x} and Si_xTe_{100-x} glasses undergo sharp, discontinuous glassy semiconductor-crystalline metal transition.

(ii) The observed properties like the semiconductor-metal transition pressure; the activation energy for electrical conduction, etc., show an anomaly at a composition $x = 20$.

(iii) The thermal crystallisation behaviour of these glasses also shows an interesting change at the composition $x = 20$.

The above results suggest that the $x = 20$ composition in Ge_xTe_{100-x} and Si_xTe_{100-x} systems should have unique structural features. Attempts are being made to explain the $x = 20$ anomaly in $A_x^{VI}B_{100-x}^{VI}$ chalcogenide glasses on the basis of a model which proposes a unique non-crystalline ordering state at $x = 20$ comprising 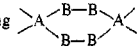 structural units.

References

1. MOTT, N. F AND DAVIS, E. A. — *Electronic processes in non-crystalline materials*, 1979, Clarendon.
2. PARTHASARATHY, G. AND GOPAL, E. S. R. — *Effect of high pressure on chalcogenide glasses*, *Bull. Mater. Sci.*, 1985, **7**, 271–302.
3. ASOKAN, S., PARTHASARATHY, G. AND GOPAL, E. S. R. — Pressure-induced-polymorphous crystallisation in bulk $Si_{20}Te_{80}$ glass, *J. Mater. Sci.*, 1986, **21**, 625–629
4. ASOKAN, S., PARTHASARATHY, G., SUBBANNA, G. N. AND GOPAL, E. S. R. — Electrical transport and crystallization studies of glassy semiconducting $Si_{20}Te_{80}$ alloy at high pressures, *J. Phys. Chem. Solids*, 1986, **47**, 341–348.
5. ASOKAN, S., PARTHASARATHY, G. AND GOPAL, E. S. R. — Evidence for a new metastable crystalline compound in Ge-Te system, *Mater. Res. Bull.*, 1986, **21**, 217–224; 1141–1142.

6. ASOKAN, S, PARTHASARATHY, G. AND GOPAL, E. S. R. Crystallization of bulk Ge_xTe_{100-x} and Si_xTe_{100-x} glasses at high pressures and temperatures, *Proc. XIV Int. Congr. on Glass*, 1986, **1**, 329–336.

7. ASOKAN, S., PARTHASARATHY, G. AND GOPAL, E S. R. Crystallization studies on bulk Si_xTe_{100-x} glasses, *J. Non-cryst. Solids*, 1986, **86**, 48–64.

8. ASOKAN, S., PARTHASARATHY, G. AND GOPAL, E. S. R. Crystallization studies on bulk Ge_xTe_{100-x} glasses, *Int. J Rapid Solidif.*, 1987, **26**, 257–271.

Thesis Abstract (Ph.D.)

Studies on laser-induced optical and morphological changes in obliquely deposited germanium and lead telluride films by L. Kameswara Rao.
Research supervisors: A Selvarajan and M. Ramakrishna Rao (ISU).
Department: Electrical Communication Engineering.

1. Introduction

Various properties of the materials, such as optical, electrical, chemical and other properties are known to be highly sensitive to their microstructure. A wide range of microstructures can be created, when the materials are prepared in thin film form, the configuration of which depends upon the preparation method as well as the experimental conditions during deposition. Oblique deposition technique is one such preparation method which is known to give rise to a characteristic tilted columnar shape to the microstructure[1]. Films possessing such microstructures are known to exhibit anomalies in their optical, electrical and physical properties which deviate by a large magnitude from the corresponding normally deposited films. Modification or removal of such a microstructure by external stimulii might result in a large variation in the optical, electrical and other properties and such variations are of scientific and technological importance, in terms of device fabrication and applications.

Laser irradiation of semiconductor films has proved to be a fruitful field for both applied and fundamental research[2]. By virtue of their ability to interact in a highly localised area and with high speed, lasers found their way into semiconductor material processing. Many interesting and reproducible material characteristics have been obtained by laser-assisted modification of the microstructure in the semiconductors.

The obliquely deposited films possess an *in situ* texture, which occurs due to nucleation and growth mechanism during deposition. Laser irradiation in such films might lead to various modifications in their properties and due to the peculiarities of the microstructure, it is expected that laser-induced effects in these films might assume a different nature as well as magnitude. The present investigations are aimed at assessing both qualitatively and semiquantitatively, the nature and magnitude of useful changes that occur in optical, structural, morphological and chemical properties of two such films, *viz.*, Ge and PbTe.

2. Experimental details

In order to investigate the films as above, two types neodimium lasers were fabricated, using mostly indigenous components. A diagnostic set-up to measure the laser parameters as well as to monitor the onset of laser-induced reactions was also fabricated and used.

The two lasers, an Nd:YAG and an Nd:glass laser, are excited by pulsed-xenon flash lamps and are operated in free running mode. Both lasers give a maximum output energy of 250 milli Joules (mj), in a pulsewidth of 300 micro seconds (ms). An energy and peak power-measuring instrument has been fabricated to monitor the laser beam parameters. A high-speed photodiode assembly with nearly a nanosecond risetime has been fabricated to monitor the pulse shape and duration. The diagnostic set-up used for investigations also facilitates detection of onset of laser-induced optical changes, time-resolved studies on photovoltage as well as time-resolved reflectivity of the sample during laser irradiation. A 20-cm focal length lens is used to focus the Nd:laser output on to the film. 3000 Å-thick films of high-purity Ge and PbTe semiconductors are used for investigations. The films are prepared at 80° angle of deposition in a vacuum of 10^{-6} Torr. The observed reactions are characterised and analysed using electron microscopy, spectrophotometry, anisotropic transmission of polarised light, laser speckle, Auger and photoelectron spectroscopy and microdensitometry.

3. Main results and conclusions

The reactions in both Ge and PbTe films are observed to proceed in two stages, classified for convenience as low- and high-beam conditions, by virtue of the difference in the nature of the observed reactions.

For Ge films, the irradiation of the films in the power density range of 9–11 Kw/cm^2, gave rise to appreciable optical transmission contrast. In the low-beam conditions, corresponding to power density near 9 Kw/cm^2, the observed contrast is nearly 7%, whereas in the high-beam conditions the observed transmission contrast is nearly 75%. The irradiated region underwent, simultaneously, structural, morphological and chemical changes. Electron microscopy studies revealed an amorphous to polycrystalline transformation. Estimation of temperature rise in the irradiated region indicated that the above transformation occurred *via* solid-phase epitaxy. Spectrophotometric data evaluation revealed that the bandgap of the material increased upon irradiation by nealy 0·1 eV. Studies on transmission of polarised light as a function of angle of incidence gave anisotropic peaking at nearly 60°, the latter being considered as approximate angle of the micrcolumns present in the film. Under low-beam conditions of irradiation, the above anisotropic nature persisted, indicating that columnar collapse is not responsible for the observed optical transmission contrast. Resistance measurements indicated an increase in effective resistance, upon irradiation which is considered as due to oxidation contamination of the film during laser heating. Time-resolved photovoltage studies showed a reversal of sign of the photovoltage in the film when the power density crossed a threshold value. An examination of Auger and XPS spectra revealed that irradiated region is enriched with GeO phase near low-beam conditions, while GeO_2 is predominantly present in high-beam conditions. Simple heating of the virgin films in ambient temperature made the film totally transparent with Ge being converted to GeO_2 phase. This enabled to prepare both positive and negative relief patterns, by suitably tailoring the irradiation conditions. It is concluded that the observed optical transmission contrast and its dependence on laser power density is essentially due to the formation of selective oxide phases, under different irradiation levels.

The PbTe films showed optical contrast effects in the power density range of 7–9 Kw/cm^2. The films exhibited a low-transmission contrast of nearly 4%, with the irradiated region becoming darkened. Relatively high-reflectance contrast of nearly 40% is observed under high-beam conditions with the irradiated region becoming relatively more transparent. The spectrophotometric data revealed that the absorption edge has shifted to longer wavelength. Electron microscopy studies revealed that the films are polycrystalline both before and after irradiation, under low-beam conditions, while the films became single crystal under high-beam conditions. Temperature estimations indicated that structural transformations occurred *via* liquid-phase epitaxy. From the nature of anisotropic

transmission of the polarised light, it is concluded that the columnar features persisted near low-beam conditions while columnar collpase has occurred under high-beam conditions. The resistance change in the film upon irradiation is negligible in the direction of vapour incidence while a slight decrease is observed in the direction perpendicular to the vapour incidence. The observations on the time-resolved photovoltage is similar to that observed in Ge films. XPS studies revealed that upon irradiation appeciable amount of TeO_2 and PbO phases are formed in the near-surface region of the film. Heat treatment of films did not reveal any interesting changes. From the above observations it is concluded that the observed transmission contrast is due to photodarkening phenomena in the irradiated region and the optical reflectance contrast under high-beam conditions is due to columnar collapse mechanism. The laser speckle studies indicated that the morphological changes in the films of both Ge and PbTe upon irradiation are mostly microscopic, with little change in the scattering characteristics of the surface.

In summary, obliquely deposited films of both Ge and PbTe exhibit optical contrast, upon laser irradiation, while undergoing, simultaneously, optical, structural, morphological and chemical changes. The mechanism responsible for contrast appearance is found to be dependent upon power density and is different for both the materials. Of the above two, Ge may be preferred for good optical transmission contrast, while PbTe films are better for high-reflectance contrast. Both negative and positive relief patterns can be registered in these films, with no additional treatment in the case of PbTe films and with heat treatment in the case of Ge films. A comparison with reported results indicates that these films have high economy of writing energy. The observed results are expected to open new avenues in the fields of optical storage, LCD displays and cold oxidation of semiconductor surfaces for device fabrication.

References

1. DIRKS, A. G. AND LEAMY, H. J. Columnar microstructure in vapor deposited thin films, *Thin Solid Films*, 1977, **47**, 219–233.

2. CULLIS, A. G. Transient annealing of semiconductors by laser, electron beam and radiant heating techniques, *Rep. Prog. Phys.*, 1985, **48**, 1155–1233.

Thesis Abstract (Ph.D.)

Effect of mechanical stress on the properties of defect levels in crystalline silicon by N. Balasubramanyam.
Research supervisor: Vikram Kumar.
Department: Physics.

1. Introduction

Study of solids under externally applied stress is useful in understanding their electronic structure as well as the fundamentals of the physical phenomena under study. Though the bulk properties of the semiconductors have been studied extensively, relatively little work has been reported on the effect of stress on impurity and defect levels. This thesis is devoted to a study of the effects of stress on some technologically important defect levels, namely, the quenched-in levels and the gold-related levels in silicon and also on meta-semiconductor interface states.

2. Experimental techniques

Current as well as capacitance-voltage measurements are done on n- and p-type Schottky barriers at various hydrostatic pressures. Deep-level transient spectroscopy[1] (DLTS) has been used for the study of the deep levels. A two-channel gated integrator-based DLTS system is used in this work. It is found[2] that the system parameters such as the gate position ratio, the gate width and the integrator response time have considerable influence on the sensitivity, resolution and accuracy of the DLTS method. Computer simulations have been used to evaluate these effects and suggestions are made for the selection of the optimum values of the parameters.

A piston-cylinder type of pressure cell is used for the application of hydrostatic pressure. The same cell is modified appropriately for the application of uniaxial stress.

3. Effect of pressure on Schottky-barrier heights

The hydrostatic pressure coefficients of the barrier heights of the Schottky contacts on n- and p-type silicon are determined. It is found that the pressure coefficient of the Schottky-barrier height in the case of n-type silicon is large and comparable to the pressure coefficient of the band gap and in the case of p-type silicon, it is small. These results indicate a pinning of the Fermi level at the surface to the top of the valence band[3]. This is in accordance with the model involving disorder-induced gap states[4] for the interface states at the metal-semiconductor contact.

4. Effect of hydrostatic pressure on deep levels in silicon

The properties of deep levels related to quenched-in defects and gold-related defects in silicon are investigated[5] under atmospheric and hydrostatic pressures. The quenched-in defects are produced by quenching silicon rapidly from high temperatures. Two levels, one at E_C-0·32 eV and the other at E_C-0.51 eV, are found in quenched n-type silicon. The capture cross-section of the shallower level decreases with temperature as T^{-2}. This is explained on the basis of an excited-state model[6] of electron capture at the defect. Both the levels move closer to the conduction band under pressure, the rate of the movement of the shallower level being slower. The capture cross-section of the shallower level increases with pressure. These levels are most likely related to iron contamination in silicon.

The properties of the gold-related acceptor (E_C-0·54 eV) and donor (E_V+0·35 eV) levels in silicon are studied under hydrostatic pressure. The pressure coefficient of the activation energy of the gold acceptor is larger than the pressure coefficient of the silicon band gap. The donor level is weakly pressure dependent. The capture cross-sections of the levels are essentially pressure independent. From the pressure coefficients of the deep levels the strain coefficients are obtained which are useful in analysing the uniaxial stress coefficients of deep levels on the basis of specific microscopic models.

5. Effect of uniaxial stress on deep levels in silicon

The uniaxial stress dependence of the parameters of the gold-related acceptor and donor levels in silicon is studied. The donor level is essentially independent of the uniaxial stress in any direction. The capture cross-sections of both the levels are stress independent. The activation energy of the acceptor level shows anisotropy in the stress coefficients. The stress coefficient in the $\langle 110 \rangle$ direction is positive whereas it is negative in the $\langle 100 \rangle$ and $\langle 111 \rangle$ directions of stress. Various microscopic models of gold-related defects in silicon are evaluated and a new model involving a divacancy-gold complex is proposed. The new model can explain the previously published data on these defects as well as the present results.

References

1. LANG, D V. — Deep level transient spectroscopy· A new method to characterize traps in semiconductors, *J. Appl. Phys.*, 1974, **45**, 3023–3032.
2. BALASUBRAMANYAM, N AND VIKRAM KUMAR — System effects in double channel gated integrator based deep level transient spectroscopy, *J. Appl. Phys.*, 1988, **64**, 6311–6314.
3 BALASUBRAMANYAM, N. AND VIKRAM KUMAR — Pressure dependence of barrier heights of Schottky contacts on silicon, *Phys. Stat. Sol. (a)*, 1987, **101**, K29–K32.
4 OHNO, H. AND HASEGAWA, H. — Correlation between the location of the interface state minimum at insulator-semiconductor interfaces and Schottky barrier heights, *Jap. J. Appl. Phys.*, 1986, **25**, L353–L356.
5. BALASUBRAMANYAM, N. AND VIKRAM KUMAR — On the quenched-in defects in *n*-type silicon, *Phys. Stat. (a)*, 1987, **100**, 239–244.

Thesis Abstract (Ph.D.)

Some studies on holographic interferometry and speckle photography by B. S. Ramprasad.
Research supervisors: E. S. Raja Gopal and P. S. Narayanan.
Department: Instrumentation and Services Unit.

1. Introduction

Holographic interferometry and its complementary technique of speckle interferometry and speckle photography have emerged as powerful techniques for the measurement of small displacements and deformations of opaque objects, besides, the measurement of changes in refractive index in phase objects. In conventional holographic interferometry applied to the measurement of deformation of opaque objects it is not often possible to measure displacements less than half a wavelength of light. Also sometimes there is an ambiguity in the interpretation of fringes. This study presents some solutions to existing problems and proceeds to demonstrate some novel applications of holographic interferometry and speckle photography. The work is divided into two parts. The first part deals with holographic interferometry and the second with speckle photography.

2. Holographic interferometry

Many of the experiments conducted centre around real-time holographic interferometry. An efficient kinematically designed liquid gate system for rapid *in-situ* processing of real-time holograms using a single solution monobath has been developed[1]. The zero fringe condition is stable over long periods of time. To measure fractional fringe displacements a holographic subtraction technique which overcomes the disadvantages of existing methods has been developed[2]. It uses a half-wave plate to introduce a phase shift of π between exposures. It has been applied to the study of the deflection of a loaded cantilever. Another technique[3] of measurement of small displacements is by introducing background fringes in double-exposed holograms (fig. 1). A thin glass wedge used as a wavefront tilter is rotated between exposures. It is shown that the displacement modulates the fringes and displacements as small as 0·07 μm can be measured. The wavefront tilter has the added advantage of eliminating phase ambiguities. This is confirmed by studying the bending of a strip. The elimination of phase ambiguity has also been achieved by a novel technique of multiplex double-exposure

FIG. 1. (a)

(b)

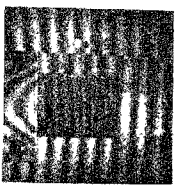

FIG. 2.

FIG. 3.

FIG. 1. Photographs of reconstructions from double-exposure holograms of the strip object with (a) no rotation of the wedge between exposures and (b) the wedge rotated by 90° between exposures.

FIG. 2. Holographic interferometry for measurement of stress and thickness of thin films combined together. The fringes on the cantilever indicate stress. The shift in the fringes at the top indicates the thickness of the film.

FIG. 3. Isothetic fringes of a strip clamped at both ends and subjected to a couple at the centre.

holographic interferometry. Multiplex hologram of a thin disc fixed around the periphery and loaded at the centre is used to demonstrate the technique.

While holographic interferometry for opaque objects deals with changes in optical path length due to deformation or displacement, holographic interferometry of phase objects deals with phase shifts due to the changes of refractive index of the medium or the thickness of the medium (fig. 2). Using real-time holographic interferometry methods have been developed to measure some of the physical parameters of thin films like the thickness, adhesion[4], intrinsic and thermal stresses.

3. Speckle photography

Speckle pattern photography is a simpler technique compared to holographic interferometry. A double-exposure specklegram is made by imaging with a lens on a high-resolution photographic plate, light scattered by an object in an undisplaced and a displaced position. Information about the displacement can be extracted by (i) Young's interference fringes obtained by illuminating the specklegram with an unexpanded laser beam or (ii) by a whole-field filtering technique.

Etch depth in metallic specimens has been studied[6] using speckle pattern photography and measurements in the range of 50 to 125 μm have been carried out. Most engineering measurements are concerned not with just displacements but strains which are derivatives of displacement. Displacement derivatives can be directly measured using defocussed speckle-pattern photography. The out-of-plane displacement of a strip has been studied theoretically and experimentally under two conditions of loading, (i) strip fixed at the longitudinal ends and loaded at the centre, (ii) strip fixed at the longitudinal ends and subjected to a bending moment. Isothetic fringes showing contours of displacement derivatives have been obtained using the whole-field filtering technique (fig. 3).

Some experiments have been conducted to demonstrate the use of speckle photography for phase objects. A novel application for testing of incandescent lamps has been described. Isothetic fringes showing changes due to the gradient of refractive index have been obtained. An interesting application of speckle photography for the measurement of changes in refractive index of liquid mixtures has been presented. It has been shown that refractive index changes even as small as 0.0005 can be measured.

References

1 HARIHARAN, P. AND RAMPRASAD, B. S. *J. Phys. E. Sci. Instrum.*, 1973, **6**, 699–701.

2 HARIHARAN, P. AND RAMPRASAD, B. S. *J. Phys. E. Sci. Instrum.*, 1972, **5**, 976–978.

3. HARIHARAN, P. AND RAMPRASAD, B. S. *J. Phys. E: Sci. Instrum.*, 1973, **6**, 173–175.

4 RAMPRASAD, B. S. AND RADHA, T. S. *Appl. Opt.*, 1978, **17**, 2670.

5. RAMPRASAD, B. S. AND RADHA, T. S *Thin Solid Films*, 1978, **51**, 335.

6. RADHA, T S. AND RAMPRASAD, B. S. *J. Electrochem. Soc. India*, 1985, **34**, 149–150.

7. RADHA, T. S. AND RAMPRASAD, B. S. *J. Electrochem. Soc. India*, 1986, **35**, 135–136.

Thesis Abstract (Ph.D.)

Investigations towards the total synthesis of natural and modified steroids by R. Saibaba.
Research supervisor: T. R. Kasturi.
Department: Organic Chemistry.

The general term 'steroids' covers all compounds containing the perhydro-1, 2-cyclopentenophenanthrene nucleus. It includes a wide variety of naturally occurring substances like sterols, bile acids, sex hormones, adrenal cortical hormones, cardiac aglycones, sapogenins and alkaloids, which possess important therapeutic properties. The pronounced physiological activity of the steroid nucleus has made it the target of numerous, often ingenious, synthetic strategies. In the total synthesis of steroids CD-hydrindane precursors can be conveniently constructed with built-in appendages for the formation of A and B rings. These intermediates can be used as potential substrates for asymmetric synthesis of steroids[1,2].

The dienealdehyde **1**, an important synthon for the total synthesis of steroids was prepared from a known[3] β-ketoester **2** in racemic and chiral forms. Thus, condensation of chloroethyl methyl ketone with 2-methylcyclopentan-1, 3-dione gave the dione **3** which on sodium borohydride reduction, hydroxyl group protection, carboxylation, followed by esterification afforded the known β-ketoester **2**. Sodium borohydride reduction of the compound **2** gave the saturated alcohol **4** resulting from conjugate hydride addition followed by the reduction of the ketone function. The same ester **2** when reduced with LAH yielded the desired allylic alcohol **5** which was oxidised to the diene aldehyde **1**. Asymmetric synthesis of the aldehyde was realised starting from the chiral β-ketoester **2**, prepared by an aminoacid-catalysed asymmetric aldol cyclisation[4].

Investigations towards developing an alternative route to the synthon **1**, *via* the intermediate **6** were also carried out. Although the desired compound **6** could not be prepared by this route, two novel products, **7** and **8**, were isolated in the course of this study. The structures of these compounds were established unambiguously by spectral (IR, ^{1}H, ^{13}C-NMR and mass) studies. An acceptable mechanism has been formulated for the formation of these two products[5].

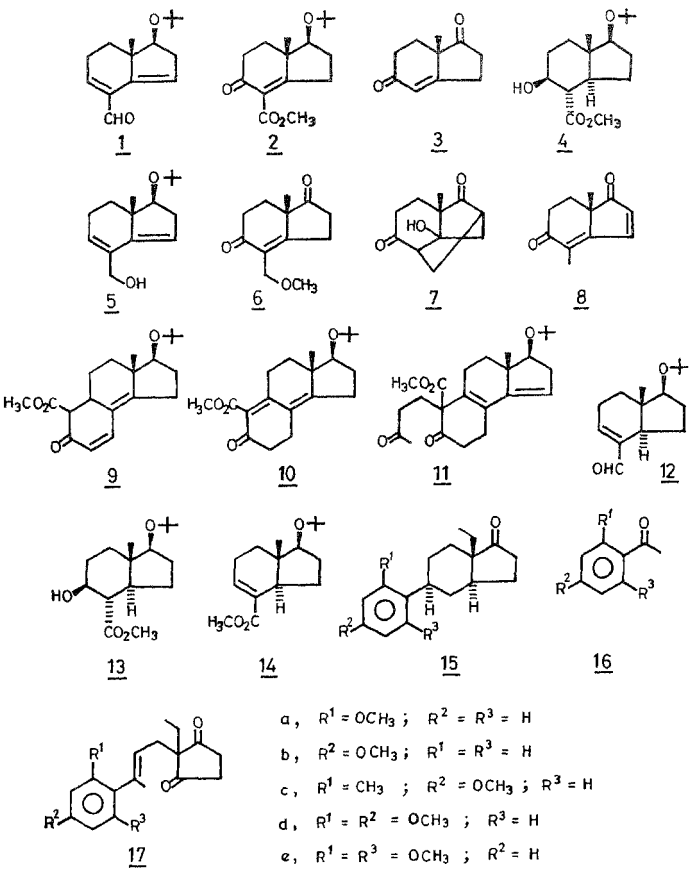

1 2 3 4 5 6 7 8 9 10 11 12 13 14 15 16 17

a, $R^1 = OCH_3$; $R^2 = R^3 = H$

b, $R^2 = OCH_3$; $R^1 = R^3 = H$

c, $R^1 = CH_3$; $R^2 = OCH_3$; $R^3 = H$

d, $R^1 = R^2 = OCH_3$; $R^3 = H$

e, $R^1 = R^3 = OCH_3$; $R^2 = H$

Annelation of the dienealdehyde **1** with methyl acetoacetate yielded the tricyclic dienone **9** which was converted to an isomeric dienone ester **10** by hydrogenation of the double bond followed by the introduction of a new double bond using selenium methodology. Condensation with methyl vinyl ketone afforded the desired alkylated product **11**.

Trans hydrindanes are of paramount importance in the total synthesis of steroids. Several methods have been developed for the synthesis of *trans* hydrindane derivatives[6]. We have successfully achieved a new synthesis of a novel synthon **12** with the *trans*-CD-ring junction, already built in, as discussed below. The β-ketoester **2** was hydrogenated and the resulting saturated ketoester was reduced to the alcohol **13**. Dehydration of the alcohol **13** to the unsaturated ester **14** was realised by conversion to corresponding mesylate followed by refluxing in DMF with NaI and pyridine. The ester **14** was transformed to the *trans*-aldehyde **12** by AlH_3 reduction followed by allylic oxidation. Starting from the optically active β-ketoester **2**, and adopting the same procedure, the aldehyde **12** was prepared in optically active form.

Many interesting biologically active B-seco-steroidal derivatives have been reported in literature. It has been shown by recent studies[7] that 13-ethyl-B-secosteroid derivatives are more potent than the corresponding methyl analogues. In view of this, various substituted 13-ethyl-B-seco-estrone analogues **15a–e** were synthesised as follows. Substituted acetophenones **16a–e**, synthesised by reported procedures, were converted to the corresponding vinyl carbinols by treatment with vinyl magnesium bromide. Condensation reactions between the vinyl carbinols and 2-ethylcyclopentan-1, 3-dione yielded the secodiones **17a–e**, which were cyclised and hydrogenated stereoselectively to the B-seco-steroids **15a–e** in excellent yields. The configuration assigned at C-9 and C-14 positions are based on a detailed proton NMR study.

References

1. AKHREM, A. A. AND TITOV, Y. A. — *Total steroid synthesis*, Plenum, 1970.
2. BLICKENSTAFF, R. T., GHOSH, A. C. AND WOLF, G. C. — *Total synthesis of steroids*, Academic, 1974.
3. MICHELI, R. A., HAJOS, Z. G., COHEN, N., PARRISH, D. R., PORTLAND, L. A., SCIAMANNA, W., SCOTT, M. A. AND WEHRLI, P. A. — *J. Org. Chem.*, 1975, **40**, 675–681.
4. HAJOS, Z. G. AND PARRISH, D. R. — *Org. Syn.*, 1985, **63**, 26–36.
5. BANERJEE, D. K., KASTURI, T. R., SAIBABA, R. AND SARKAR, A. — *Proc. Indian Acad. Sci. (Chem. Sci.)*, 1985, **95**, 439–446.
6. COHEN, N. — *Acc. Chem. Res.*, 1976, **9**, 412–417.
7. JHINGRAN, A. G., GUPTA, R. C., RAY, S., AGARWAL, A. K., SINGH, M. M. AND NITYA ANAND — *Steroids*, 1983, **42**, 627–634.